J Neurophysiol 89: 355–366, 2003.
10.1152/jn.00058.2002.

Eye Movements During Multi-Axis Whole-Body Rotations

CHRISTOPHER J. BOCKISCH,[1] DOMINIK STRAUMANN,[1] AND THOMAS HASLWANTER[1,2]
[1]*Department of Neurology, University Hospital Zürich, CH-8091 Zürich; and* [2]*Institute of Theoretical Physics, Eidgenössische Technische Hochschule, CH-8093 Zürich, Switzerland*

Submitted 30 January 2002; accepted in final form 4 September 2002

Bockisch, Christopher J., Dominik Straumann, and Thomas Haslwanter. Eye movements during multi-axis whole-body rotations. *J Neurophysiol* 89: 355–366, 2003. 10.1152/jn.00058.2002. The semicircular canals and the otolith organs both contribute to gaze stabilization during head movement. We investigated how these sensory signals interact when they provide conflicting information about head orientation in space. Human subjects were reoriented 90° in pitch or roll during long-duration, constant-velocity rotation about the earth-vertical axis while we measured three-dimensional eye movements. After the reorientation, the otoliths correctly indicated the static orientation of the subject with respect to gravity, while the semicircular canals provided a strong signal of rotation. This rotation signal from the canals could only be consistent with a static orientation with respect to gravity if the rotation-axis indicated by the canals was exactly parallel to gravity. This was not true, so a cue-conflict existed. These conflicting stimuli elicited motion sickness and a complex tumbling sensation. Strong horizontal, vertical, and/or torsional eye movements were also induced, allowing us to study the influence of the conflict between the otoliths and the canals on all three eye-movement components. We found a shortening of the horizontal and vertical time constants of the decay of nystagmus and a trend for an increase in peak velocity following reorientation. The dumping of the velocity storage occurred regardless of whether eye velocity along that axis was compensatory to the head rotation or not. We found a trend for the axis of eye velocity to reorient to make the head-velocity signal from the canals consistent with the head-orientation signal from the otoliths, but this reorientation was small and only observed when subjects were tilted to upright. Previous models of canal-otolith interaction could not fully account for our data, particularly the decreased time constant of the decay of nystagmus. We present a model with a mechanism that reduces the velocity-storage component in the presence of a strong cue-conflict. Our study, supported by other experiments, also indicates that static otolith signals exhibit considerably smaller effects on eye movements in humans than in monkeys.

INTRODUCTION

Successful execution of goal-directed movements depends on the accurate perception of our orientation, movement, and the location of the objects around us. To achieve this, the CNS integrates information from the semi-circular canals about head angular velocity, linear acceleration information (translation and gravity) from the otolith organs, proprioception, and vision. Behavioral responses to external stimuli depend on our orientation with respect to gravity: for example, if we lean forward, we have to make a step or shift our weight to keep from falling over. There are indications that, at least in monkey, the angular vestibular ocular reflex (aVOR) is also modified by gravity (reviewed in Cohen et al. 1999).

Simultaneous stimulation of the semi-circular canals and a change in otolith signals occurs frequently, such as when walking around a corner (Imai et al. 2001). In most situations, the otoliths and the semicircular canals produce consistent responses. For example, when a person is upright and the head then tilts to the side or forward, the semi-circular canals indicate the angular rotation, and the otoliths signal the change of head position relative to gravity. Such dynamic otolith signals assist the aVOR during passive head roll: Schmid-Priscoveanu et al. (2000) found that torsion gain during head roll is higher when the head is upright compared with when the head is supine. In addition, during low-frequency oscillation when only the canals are stimulated, peak eye velocity occurs prior to peak head velocity (a "phase lead"), but this phase asynchrony is decreased by simultaneous, consistent otolith stimulation. The otoliths themselves are capable of generating a head-rotation signal to produce nystagmus. During sustained off-vertical axis rotation (for example, "barbecue-spit" rotation), eye movements compensatory for the head rotation occur long after the vestibular signal from the semicircular canals has decayed and presumably are derived from the dynamic otolith signal (Angelaki and Hess 1996; Darlot et al. 1988; Haslwanter et al. 2000; Harris 1987; Hess and Dieringer 1990; Raphan et al. 1981).

Inconsistent canal and otolith signals indicate the presence of disease or injury and can also occur in extreme environments such as micro- or hypergravity. There is considerable evidence that in monkey the otolith signals modify the interpretation of canal signals driving the aVOR. For example, if a monkey is tilted shortly after the cessation of long duration constant-velocity rotation, the axis of postrotatory nystagmus tends to align with gravity, showing a tendency for the axis of eye velocity to remain stable in space (Angelaki and Hess 1994; Merfeld et al. 1993b). In these studies, the head-velocity signals from the canals are inconsistent with the static otolith signal: after a postrotatory reorientation from upright to ear down, the canals signal a yaw head rotation, whereas the otoliths indicate that the head is constantly ear-down. The monkey nervous system adjusts to this conflict by reinterpreting the head-velocity signal (yaw head velocity from the canals converted to pitch eye velocity) so that it is consistent with the otolith signal. In humans, the dependence of eye velocity on

Address for reprint requests: C. J. Bockisch, Dept. of Neurology, Univ. Hospital Zürich, Frauenklinikstr. 26, CH-8091, Zürich, Switzerland (E-mail: Chris.Bockisch@nos.usz.ch).

The costs of publication of this article were defrayed in part by the payment of page charges. The article must therefore be hereby marked "*advertisement*" in accordance with 18 U.S.C. Section 1734 solely to indicate this fact.

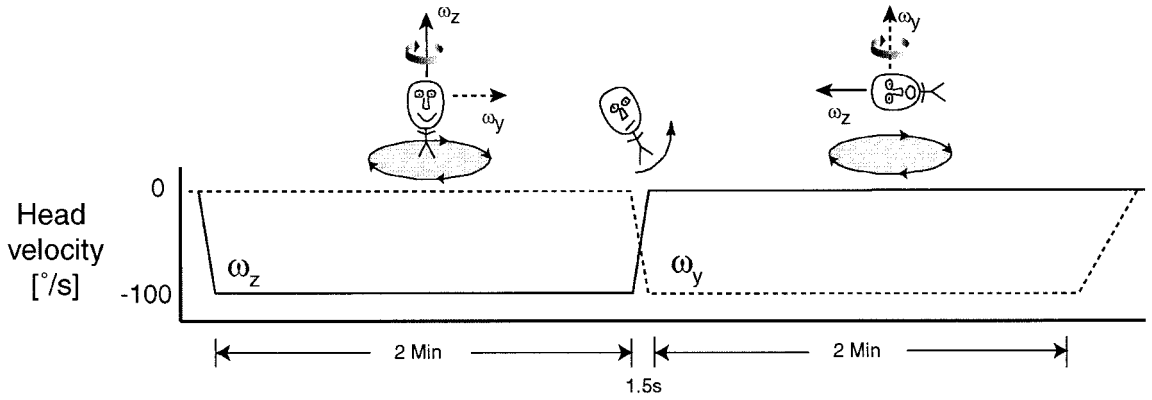

FIG. 1. Trial schema when subjects were reoriented from upright to right ear down during −100°/s rotation about the earth-vertical axis. Subjects were seated on a platform (represented by the gray circles) that rotated at −100°/s continuously throughout the trial (the direction is represented by the arrows on the platform). While the platform continued to rotate, the direction of head rotation changed due to the 90° reorientation that occurred 2 min into the trial. As a result of the reorientation, rotation about the head-yaw axis changed from −100 to 0°/s (ω_z and solid lines), while rotation about the head-pitch axis (ω_y and dotted lines) changed from 0 to −100°/s. The duration of the reorientation is exaggerated for clarity.

gravity during postrotatory tilts is smaller (Fetter et al. 1992). In static conditions, the otoliths also exert less influence on three-dimensional (3D) eye position in human than in monkey (Bockisch and Haslwanter 2001).

We investigated the effect of otolith-canal interactions on 3D eye movements with a unique stimulus that produces a powerful cue conflict. We took advantage of a property of the peripheral vestibular system that makes it insensitive to long-duration, constant-velocity rotation about the earth-vertical axis. Endolymph flow in the vestibular labyrinth, which causes bending of the hair cells in the ampulla and subsequent neural firing in the vestibular nerve, is caused by head acceleration (Hain et al. 2000). The high viscosity of the endolymph mechanically converts the acceleration signal into a signal that initially is approximately proportional to head velocity. For longer-duration rotations, however, the mechanical elasticity of the cupula starts to act and pulls the cupula back to the resting position (Wilson and Melvill-Jones 1979). As a result, during a prolonged constant-velocity rotation, the vestibular canals signal a head rotation only for the first 30–60 s.[1] After that, subjects experience no feeling of rotation. A subsequent deceleration is therefore perceived as acceleration in the opposite direction ("postrotatory" responses). Our paradigm makes use of this phenomenon, as shown in Fig. 1. We rotated subjects about the earth-vertical axis at a constant velocity for 2 min (Fig. 1, *left*), allowing the response from the canals and the vestibular neurons to decay. While the constant velocity rotation continued, we reoriented subjects 90°, in this example from an upright position onto their right side (Fig. 1, *middle*). After the reorientation, *acceleration* about the inter-aural axis (ω_y increases from 0 to −100°/s) produces appropriate responses from the vertical canals, whereas the *deceleration* about the head-yaw axis (ω_z decreases from −100°/s to 0) also stimulates the horizontal canals (the postrotatory response described in the preceding text). Note that the response from the horizontal canals is not compensatory for the head rotation because after the rotation the subject only rotates about the interaural *y* axis. After the reorientation, the otolith organs, which signal head orientation relative to gravity, indicate correctly that the head is right-ear down and therefore contradicts the signal from the horizontal canals. Our experiments test how the brain responds to this otolith-canal cue conflict.

Only a few models describing otolith-canal interaction for complex movements in three dimensions exist. A popular model was developed by Merfeld (Merfeld et al. 1993a) and has been used to simulate the responses in monkeys as well as in humans (Glasauer and Merfeld 1997; Merfeld 1995). This model, in which a head-rotation signal is derived from a mismatch between expected and experienced otolith signals, successfully fits eye movements after postrotatory tilts (Merfeld et al. 1999), and— in a slightly modified version—also eye movements produced by off-vertical axis rotations (OVAR) (Haslwanter et al. 2000). When these models failed to reproduce our experimental findings, we investigated which changes were necessary to get a good agreement between model and data.

Portions of this work have been presented previously in abstract form (Bockisch and Haslwanter 2001; Bockisch et al. 2001a,b).

METHODS

Subjects

Our seven healthy volunteers, including the authors, averaged 33 yr of age (range: 26–41) and were free of any known vestibular or ocular pathologies. They were informed of the potentially nauseating effects of the stimulus prior to the experiment and were allowed to stop the experiment at any time. The experimental protocols were approved by a local ethics committee at Zürich University Hospital, and adhered to the Declaration of Helsinki for research involving human subjects.

Apparatus

The 3D human turntable at the Dept of Neurology, Zürich, used for these experiments is driven by three servo-controlled motorized axes (Acutronic, Switzerland), controlled with Acutrol software and hardware, and interfaced with LabVIEW software. All axes needed for this paradigm can be accelerated at 160°/s^2 or more.

[1] More specifically, the cupula returns to the resting position with a time constant of ~7 s, i.e. after 7 s the deflection of the cupula has decreased by 1/*e* (= 63%). A central neural processing mechanism called "velocity storage" extends this time constant for horizontal rotations to ~20s (Raphan et al. 1979).

Subjects were comfortably seated in a chair and secured with safety belts, and evacuation pillows were molded to the upper body and legs. The center of the head was positioned at the center of rotations. Individually adjusted masks (Sinmed BV, Reeuwijk, The Netherlands), made of a thermoplastic material (Posicast), were molded to the contour of the head after warming, with openings in the mask made for the eyes and mouth. The mask was attached to the back of the chair and very effectively restricted head movements without causing discomfort.

Subjects viewed with both eyes, and the 3D position of the left eye was measured with search coils manufactured by Skalar (Delft, The Netherlands). The head was surrounded by a chair-fixed coil frame (side length: 0.5 m) that produced three orthogonal magnetic fields with frequencies of 80, 96, and 120 kHz. The signals were amplified and multiplexed before passing through the turntable slip rings. A high-performance digital signal processor computed a fast Fourier transform in real time on the digitized search coil signal to determine the voltage induced in the coil by each magnetic field (system manufactured by Primelec, Regensdorf, Switzerland). The orientation of the coil could be determined with an error of $<7\%$ over a range of $\pm 30°$ and with a noise level of $<0.05°$ (root-mean-squared deviation). Eye position signals were digitized with 12-bit accuracy and chair position signals with 16-bit accuracy. All data were sampled at 1 kHz and analyzed off-line with MatLab software (The MathWorks, Boston MA).

Details of our search coil calibration procedure are given elsewhere (Straumann et al. 1995). Briefly, we zeroed voltage offsets while placing the search coils in a metal tube to shield them from the magnetic fields. Then we measured the relative gains of the three magnetic fields with the search coils on a gimbal system placed in the magnetic field at the same location as the measured eye.

Procedure

All experiments were conducted in the dark. Between trials, the room lights were turned on while the subject was upright.

Reorientation experiments

We reoriented subjects 90° in roll or pitch during constant-velocity rotation about the earth-vertical axis. In separate experiments, subjects were reoriented from upright to right-ear down (RED), right-ear down to upright, upright to supine, and supine to upright. We refer to the upright-to-RED and RED-to upright conditions as "roll reorientation" experiments and the upright-to-supine and supine-to-upright conditions as "pitch reorientation" experiments.

Subjects were accelerated about the earth-vertical axis up to a constant velocity of 100°/s. After allowing 2 min for canal responses and eye velocity to decline, subjects were reoriented 90° in 1.54 s (i.e., a velocity triangle with $152°/s^2$ acceleration), while earth-vertical axis rotation continued for an additional 2 min (see Fig. 1). Subjects were instructed to keep their eyes open throughout the trial but to not try and "fixate" anything in particular. Following each trial, subjects were asked to describe their perceived body orientation and movement after the reorientation.

The direction of earth-vertical axis rotation was chosen such that the direction of the initial nystagmus expected from the canal stimulation after reorientation was the same in all conditions, thus controlling for the possibility of directional asymmetries of nystagmus (right vs. left, up vs. down, or clockwise vs. counterclockwise). For example, earth-vertical axis rotation was toward the right ear in the upright-to-RED condition, producing primarily rightward and downward slow phases after reorientation (see Fig. 1). Earth-vertical axis rotation was in the opposite direction in the RED-to-upright condition, likewise producing right- and downward nystagmus. Similar procedures were used for the upright-to-supine and supine-to-upright conditions to produce primarily rightward and clockwise eye movements in both conditions.

Four subjects completed all protocols, two additional subjects participated in the roll reorientation experiment, and one additional subject completed the pitch experiment.

Control experiments

For comparison, we recorded eye movements when subjects were accelerated about an earth-vertical axis at $65°/s^2$ to 100°/s without reorientation (a simple velocity step) while upright, RED, or supine. Thus the acceleration time in control trials was the same (1.54 s) as the reorientation period.[2] To compare the contribution of the individual canals to the actually observed eye movements, we calculated the simple linear addition of the eye-movement responses to the velocity steps, e.g., upright-to-supine = upright + supine. Interactions between the different canal and otolith signals would show up as deviations of the observed eye movements from this simple linear addition. For the prediction, we added the slow phase eye velocity from the control trials in all three axes (horizontal, vertical, and torsional). The effect of the otolith-canal cue conflict can then be determined by comparing the sum-of-control data with the reorientation data.

Subjects completed the upright-to-RED and RED-to-upright as well as the associated control procedures in a single session. Upright-to-supine, supine-to-upright, and their control trials were conducted in a separate session. All subjects finished the control procedures prior to the reorientation procedures. Subjects who did not complain of nausea completed a second set of control trials at the end of the experiment, to control for any adaptation effects. Two subjects in the roll and one subject in the pitch reorientation experiment opted not to continue with additional control trials. Because the second set of control trials was statistically equivalent to the first (determined by *t*-test), we report their average.

Data analysis

We represent eye positions as 3D rotation vectors in a right-handed, head-fixed coordinate system. Positive eye position values indicate clockwise, down, and left from the subject's perspective. We call rotation around the naso-occipital axis "torsion" and distinguish it from rotation about the line-of-sight. (In these experiments, gaze direction was generally close to straight ahead, where torsion in a head-fixed coordinate system is similar to rotation about the line-of-sight.) Likewise, we refer to rotations about the interaural axis as "vertical" eye movements, and rotations about the axis pointing through the top of the head as "horizontal" eye movements. We use "eye position" to refer to 3D eye position in head-fixed coordinates. The reference position for computing the rotation vectors, corresponding to 0° horizontally, vertically, and torsionally, was always determined by the eye position when the subject was upright and fixating a 1.5-m distant target in the mid-sagittal plane prior to the start of each trial.

Rotation vectors were smoothed, and angular eye velocity was computed as described previously (Hepp 1990; Tweed et al. 1990). Slow phase eye velocity was found by an interactive computer program that began by computing the median between zero crossings in the eye velocity (Straumann 1991). Next, the maximum duration of the intervals (long slow phases uninterrupted by saccades, e.g., 300 ms or more) could be split into shorter-duration pieces (e.g., 100 ms),

[2] We simulated the canal response to both acceleration profiles, assuming the canal transfer function can be described by a single time constant of 4.5 s. Because the time constant of the canals is significantly larger than the acceleration period, the maximum difference in the peripheral responses was $<3\%$ of the response signal. Canal time constants >4.5 s, or any kind of velocity storage, led to even smaller differences.

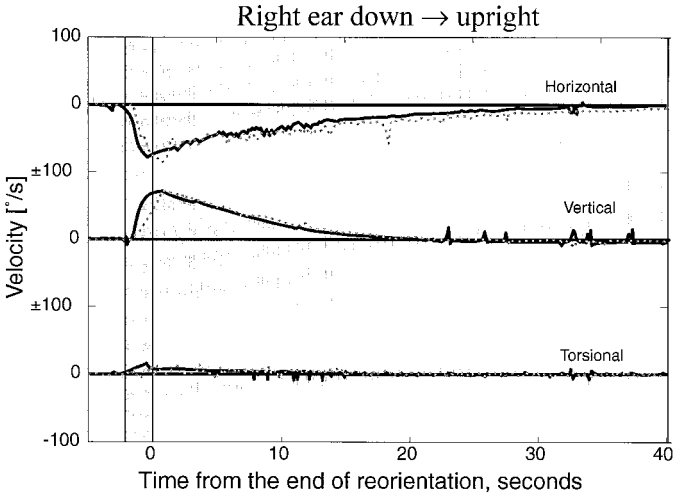

FIG. 2. Eye movements for 1 subject following reorientation from right-ear down-to-upright. Gray lines are eye velocity (truncated at ± 100°/s), the thick line is the desaccaded eye velocity, the gray bar marks the reorientation period, and the dotted line is the summed desaccaded velocity from the corresponding control trials (velocity steps without reorientation).

and medians computed separately for each piece. Short intervals between zero crossings (saccades, <80 ms) were ignored. Finally, we linearly interpolated between the median velocity points. The quality of the saccade removal was checked visually, and examples of our desaccading procedures can be seen in Fig. 2. To estimate peak velocity and the decay of nystagmus, we fit single exponential curves to the slow-phase eye velocity.

Eye-position dependency of the VOR

The human VOR is known to vary with gaze direction. Misslisch (Misslisch and Tweed 2001; Misslisch et al. 1996) has described the eye-position-dependent modulation of the VOR as a compromise between a perfect VOR, where eye velocity would be equal in speed but opposite in direction to the head velocity, and adherence to Listing's Law (Helmholtz 1867), which puts a restriction on the allowed axes of eye velocity: for the eye position to remain in Listing's Plane for different gaze directions, the axis of eye velocity must tilt by half the gaze angle (Haslwanter 1995; Tweed and Vilis 1990). The compromise between a perfect VOR and Listing's Law means that during yaw and pitch head rotation, the axis of eye velocity tilts by approximately one-quarter, not one-half, the gaze angle. During torsional VOR, the angular velocity axis tilts in the opposite direction to the gaze line by about half the angle (Misslisch et al. 1994). In other words, eye velocity along axes different from the head velocity axis can be induced by changes in eye position. Because we did not measure Listing's Plane in our subjects, we investigated a possible correlation between eye position and torsional eye velocity by computing the mean eye positions (we first smoothed individual subject data with a 2-s moving average window) to determine if there was any systematic variation in eye position in our conditions.

RESULTS

Sum-of-control trials

Control trials were performed with velocity steps of 100°/s about the earth vertical axis when subjects were upright, RED, or supine. They produced eye velocity primarily confined to the axis of head rotation. We sometimes found small (~5°/s), idiosyncratic, misalignments of the axis of eye velocity with the axis of head rotation. Small misalignments during rotation about an earth vertical axis were also reported by Haslwanter et al. (1996) and Tweed et al. (1994).

Nystagmus in the plane of the head rotation was similar to that reported by others. We found, on average, in the sum-of-control trials, peak rightward velocity of 46.9°/s, which decayed with a time constant of 14.6 s for the roll-reorientation experiment, and 42.6°/s (17.1 s) for the pitch-reorientation experiment. The average peak downward velocity was 50.3°/s and decayed with a time constant of 7.1 s (subjects RED). And the average peak clockwise velocity was 31.6°/s, and decayed with a time constant of 5.4 s (subjects supine).

Reorientation

Reorientation during earth-vertical axis rotation was extremely disorienting and produced an initial tumbling sensation that sometimes was accompanied with a perception of body tilt. Subjects typically reported that the perceived reorientation was >90°. For example, some subjects reported that after moving from upright to RED, they initially felt that their feet were higher than their head. The percept of body orientation would usually return to normal in 30–60 s. Our subjects sometimes reported other body movement illusions, which is consistent with reports of large inter-subject differences in perceived tilt during active head rotations on a short axis centrifuge (Hecht et al. 2001).

Roll reorientation

Reorienting subjects 90° in roll during earth vertical axis rotation generated strong horizontal and vertical slow-phase eye velocity, as expected from the stimulation of the semicircular canals. Figure 2 shows typical eye velocity after reorientation from RED to upright in one subject. As with other subjects, horizontal eye velocity decayed slower than vertical eye velocity. This subject also showed a small amount of torsional nystagmus (maximum 8°/s), which was only occasionally observed in our subjects. After the reorientation, the subject was upright and still rotating about an earth-vertical axis, so compensatory eye velocity would only be horizontal. Nonetheless, this subject still showed strong vertical nystagmus, which is inconsistent with otolith information indicating, correctly, that head orientation relative to gravity was not changing. Figure 2 also shows that the summed data for the control conditions in this subject (i.e., the sum of the eye velocities during upright and RED rotation about an earth vertical axis, dotted lines) was very similar to the reorientation data.

As can be inferred from Fig. 2, the direction of eye velocity did not rapidly reorient to align with the axis of head rotation. This was true for all our subjects. The *direction* of eye velocity is easier to appreciate by plotting vertical against horizontal eye velocity, and the average data of six subjects are shown in Fig. 3. The figure shows 30 s of data beginning 1 s after the end of reorientation. (Slow-phase eye velocity was usually difficult to identify immediately after reorientation.) In the RED-to-upright condition, compensatory eye rotation would be horizontal, yet we see that the direction of eye velocity is similar to the sum-of-control conditions, as well as to the upright-to-RED condition where purely vertical eye velocity would have been compensatory to the head rotation. Figure 3 *B*, and *C*, also

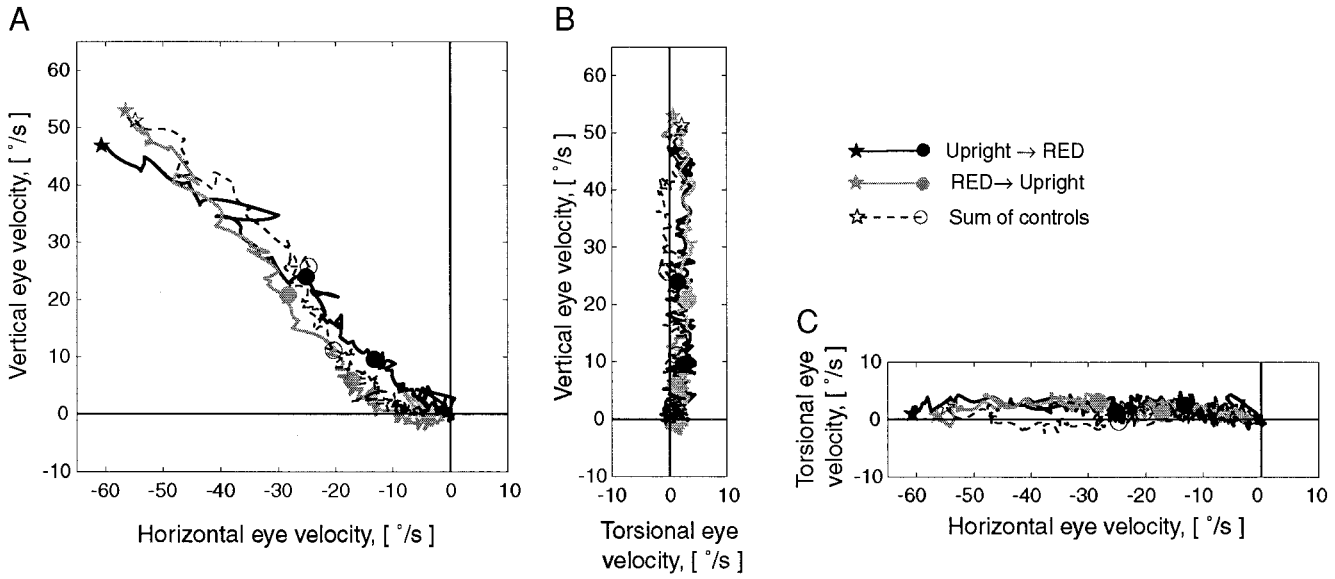

FIG. 3. Slow phase eye velocity, averaged over 6 subjects, is shown for upright-to-RED , (black lines), RED-to- upright, (gray lines), and sum of control conditions (dashed lines). Thirty seconds of data are shown in each condition. *A*: vertical vs. horizontal eye velocity. Stars mark the first analyzed data points, 1 s after the end of reorientation, and circles mark points 5 and 10 s later. *B*: vertical vs. torsional eye velocity. *C*: torsional vs. horizontal eye velocity.

shows that, on average, our subjects tended to have clockwise torsional eye velocity in both reorientation conditions but not in the control conditions.

In the upright-to-RED condition, average peak eye velocity, as determined by the exponential fits, was 52.2 and 61.6°/s for vertical and horizontal eye velocity, respectively (Fig. 4*A*). In the RED-to-upright condition, average peak eye velocity was 59.4 and 53.6°/s for vertical and horizontal eye velocity, respectively.

Horizontal time constants tended to be longer than vertical time constants (Fig. 4*B*). On average, we found horizontal time constants of 14.6, 6.8, and 9.8 s for sum-of-control, upright-to-RED and RED-to-upright conditions, respectively. Vertical time constants were 7.2, 5.7, and 4.5 s for sum-of-control, upright-to-RED, and RED-to-upright conditions, respectively.

An estimate of the effect of the canal-otolith cue conflict can be obtained by comparing the reorientation data with the sum-of-control data. We subtracted, within each subject, the fitted parameters of sum-of-control trials from those of reorientation trials. Because the data from upright-to-RED and RED-to-upright were similar, we combined the data. Horizontal peak velocity tended to be higher in the reorientation conditions (Fig. 4*A*). Collapsed across reorienting condition, the mean difference, 10.7°/s, did not quite reach statistical significance ($t = 2.1$, $P = 0.06$; $df = 11$). Vertical peak velocity after reorientation was on average 5.5°/s faster than sum-of-control trials; this was not statistically significant ($t = 1.9$, $P < 0.1$, $df = 11$). So for both horizontal and vertical eye velocity, there was a trend for peak velocity to be higher in reorientation compared with sum-of-control trials.

Time constants were generally lower during reorientation trials, particularly for horizontal eye movements (Fig. 4*B*). The average horizontal time constant, collapsed across reorientation condition, was 6.3 s shorter than the time constants in sum-of-control condition (paired $t = 4.6$; $P < 0.01$; $df = 11$). Vertical time constants after reorientation were, on average, 2.0 s shorter then the sum-of-control condition (paired $t = 2.6$, $P < 0.05$; $df = 11$).

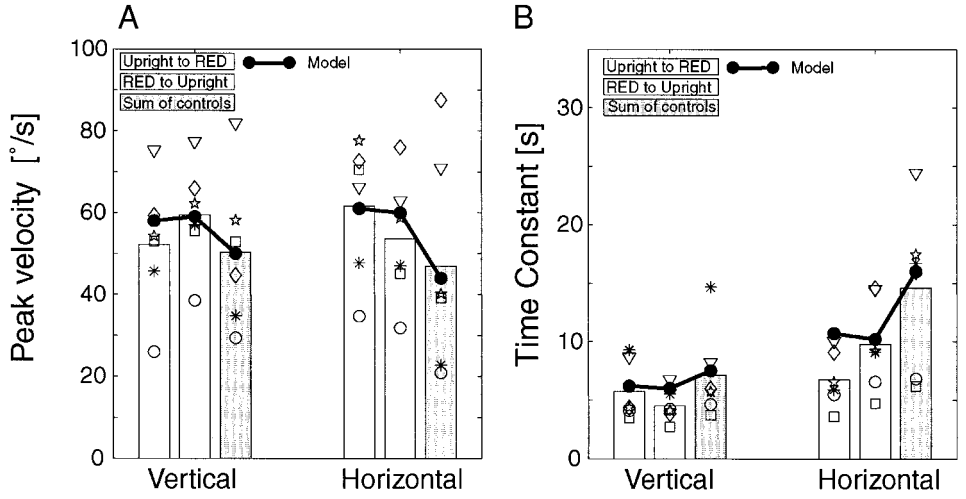

FIG. 4. Peak velocity (*A*) and the time constant of the decay of nystagmus (*B*) for roll reorientation and sum of control trials. Open points are individual subjects, and the bars are their means. Solid points are model results, with connecting lines for clarity only (see text for model details).

In Fig. 3*A*, it is apparent that in the RED-to-upright condition vertical velocity drops to zero faster than horizontal velocity, which produces a curvature in the spatial plot after 10 s. This appears consistent with postrotatory tilt studies in monkeys (Angelaki et al. 1994; Merfeld et al. 1993b). Curvature in the opposite direction for the upright-to-RED condition was not apparent. To test if reorientation of the axis of eye velocity did occur, we compared the ratio of horizontal-to-vertical time constants in our two conditions ($\tau_{horizontal}/\tau_{vertical}$). If reorientation occurs, the ratio would be higher in the RED-to-upright condition. Comparing the ratios in the two conditions allows us to test for curvature, independent of any shortening of the time constants that is not specific to the direction of reorientation. The mean ratios were 2.19 ± 0.83 (mean ± SD) in the RED-to-upright condition and 1.29 ± 0.49 in the upright-to-RED condition. While the difference (0.9) was not significant with a paired *t*-test ($t = 1.9$, $P < 0.12$, $df = 5$), the ratios for all six subjects were higher in the RED-to-upright condition.

Torsional eye velocity immediately after both reorientation and control trials was idiosyncratic. On average, mean torsional velocity after reorientation was about zero but then increased over the next several seconds (Fig. 3, *B* and *C*). Three subjects showed clockwise torsion (~10°/s) in both reorienting conditions, while the remaining subjects showed torsion in neither reorienting condition. Most subjects, including all of the subjects who did not have torsional nystagmus in the reorienting conditions, showed clockwise torsion in the upright control condition [consistent with the findings by Haslwanter et al. (1996)], and counterclockwise torsion in the RED control condition. Because torsional eye movements can be produced during yaw and pitch head movements when the gaze direction deviates from primary position, the inconsistent torsional movements could have been due to changes in gaze direction (Misslisch and Hess 2000; Misslisch et al. 1996, 2001). We checked for this possibility, by determining the average eye position for control, upright-to-RED, and RED-to-upright conditions. However, as Fig. 5 shows, the horizontal and vertical eye positions were similar and close to straight ahead.

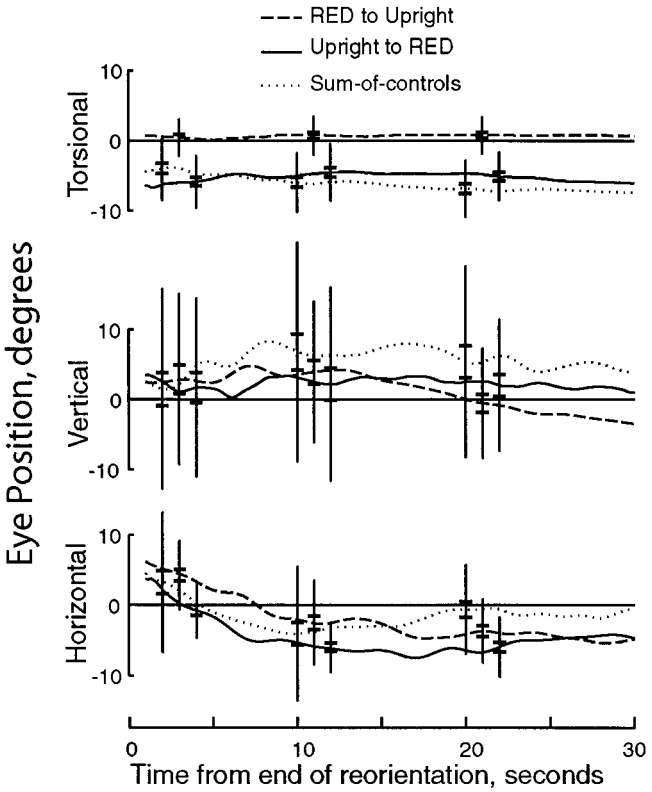

FIG. 5. Mean eye position for 6 subjects after roll reorientation. Torsional, vertical, and horizontal eye positions for individual subjects were first smoothed with a 2-s moving average. Error bars are ±1 SD, and tick marks show the SE.

Pitch reorientation

Ninety-degree pitch reorientation during earth vertical axis rotation produced strong rightward nystagmus and smaller clockwise nystagmus. Figure 6 shows the average data of five subjects. In the upright-to-supine condition, eye movements compensatory to the rotation would be torsional, yet we found considerable horizontal eye velocity, presumably caused by the postrotatory response in the horizontal canals. Likewise, in the supine-to-upright condition, horizontal eye movements were compensatory for the earth-vertical axis rotation while the subject was upright, yet torsional velocity was observed. On average, we saw little consistent vertical eye velocity.

Average peak horizontal eye velocity, as determined by exponential fits, was 42.6, 49.3, and 60.3°/s for sum-of-control, upright-to-supine, and supine-to-upright conditions, respectively (Fig. 7). Mean peak torsional eye velocity was 31.6, 37.8, and 41.0°/s for sum-of-control, upright-to-supine, and supine-to-upright conditions, respectively.

Horizontal peak velocity tended to be larger in the reorientation conditions compared with the sum-of-control condition. Collapsed across reorientation condition, the average horizontal peak velocity was 12.2°/s faster in reorientation conditions compared with the sum-of-control condition, although this difference was not quite statistically significantly different from zero ($t = 2.1$, $P = 0.07$, $df = 9$). Collapsed across reorientation condition, the average torsional peak velocity was 7.8°/s faster than in the sum-of-control condition ($t = 3.27$, $P < 0.01$; $df = 9$).

Horizontal eye velocity decayed slower than torsional eye velocity. Mean horizontal time constants were 17.1, 7.7, and 10.8 s for sum-of-control, upright-to-supine, and supine-to-upright conditions, respectively. Combining the reorientation conditions, the average time constant after reorientation was 7.8 s shorter than sum-of-control conditions ($t = 3.3$; $P < 0.01$; $df = 9$). Mean torsional time constants were 5.4, 5.3, and 5.0 s for sum-of-control, upright-to-supine, and supine-to-upright conditions, respectively, and the average torsional time constant in the sum-of-control condition was not significantly different from reorientation trials.

Figure 6*A* shows that in the supine-to-upright condition, eye velocity bends toward horizontal, but the upright-to-supine shows little curvature. This result is similar to the roll reorientation experiment, where eye velocity bends toward horizontal when subjects are reoriented to upright. We tested the significance of the curvature by comparing the ratio of horizontal-to-torsional time constants in our two conditions ($\tau_{horizontal}/\tau_{torsional}$). The average ratios were 2.77 ± 1.74 in the supine-to-upright condition, and 1.21 ± 0.92 in the upright-to-

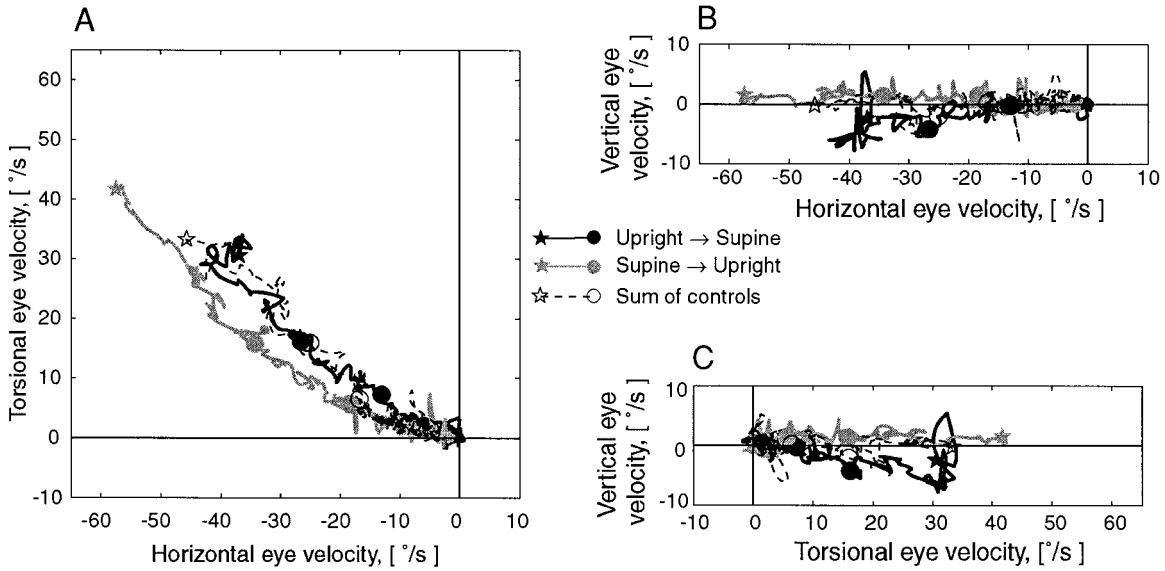

FIG. 6. Slow phase eye velocity, averaged over 5 subjects, is shown for upright-to-supine (black lines), supine-to-upright, (gray lines), and sum-of-control conditions (dashed lines). Thirty seconds of data are shown in each condition. *A*: torsional vs. horizontal eye velocity. Stars mark the first analyzed data points, 1 s after the end of reorientation, and circles mark points 5 and 10 s later. *B*: vertical vs. horizontal eye velocity. *C*: vertical vs. torsional eye velocity.

supine condition. The difference (1.56) was significant in a paired *t*-test ($t = 3.28$, $P < 0.05$, df = 4).

Mean eye positions after reorientation are shown in Fig. 8, and the upright-to-supine, supine-to-upright, and control conditions were similar, so the differences in peak velocity and time constants are not due to variations in eye position.

Otolith-canal interaction model

We simulated the eye movement responses to the combined stimulation of the semicircular canals and the otoliths in our experiments using Matlab and Simulink software (The MathWorks). We first tested our reorientation paradigm with the otolith-canal interaction model of Haslwanter, Jaeger, Mayr, and Fetter (Haslwanter et al. 2000). This model, which builds on an earlier suggestion by Merfeld (Merfeld 1995; Merfeld et al. 1993a), successfully predicts responses to linear accelerations in arbitrary directions, to rotations about different static and dynamic axes, and to interactions between canal and otolith responses during OVAR.

Figure 9 shows our current model, and elements that have been changed with respect to Haslwanter et al. (2000) have a *black shadow*. Both models are based on two negative feedback loops (gray dashed arrows in Fig. 9), one processing angular velocity signals measured by the semicircular canals (Fig. 9, *bottom*) and one processing signals from the otoliths (Fig. 9, *top*). The model also assumes that an estimate of head velocity is derived from the otolith signals by comparing the expected direction of the gravito-inertial force to the actually experienced one (indicated by $\times$ in Fig. 9), which is coupled to the vestibular velocity storage mechanism. This cross coupling is necessary to produce horizontal nystagmus during OVAR (Haslwanter et al. 2000).

While the original model exhibited responses that were qualitatively similar to the ones observed in the experimental data, particularly for the spatial response as in Figs. 3 and 6, it failed to reproduce the different gains for rotations about the horizontal, vertical, and torsional axes. It also did not reproduce the shortening of the decay of the eye-movement response

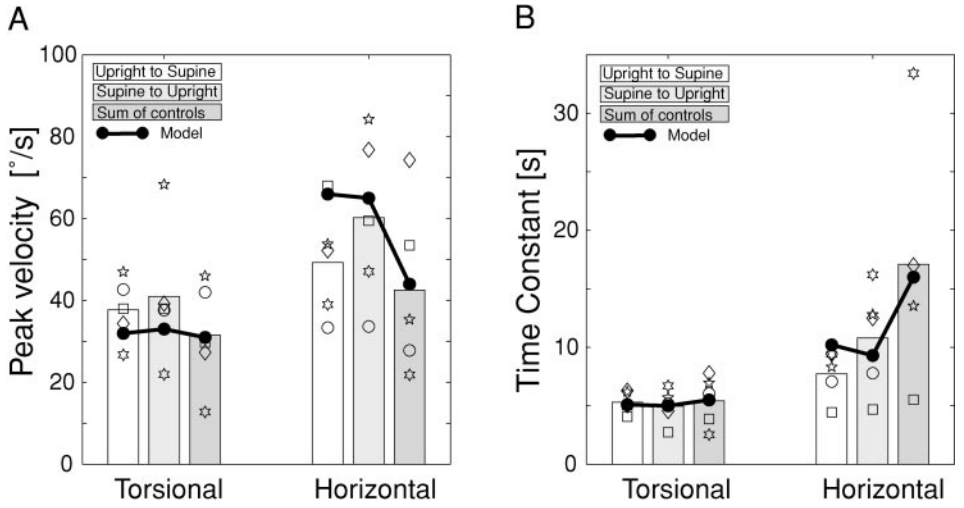

FIG. 7. Peak velocity (*A*) and the time constant of the decay of nystagmus (*B*) for pitch reorientation and sum-of-control conditions. Open points are individual subjects, and the bars are their means. Solid points are model results, with connecting lines for clarity only (see text for model details).

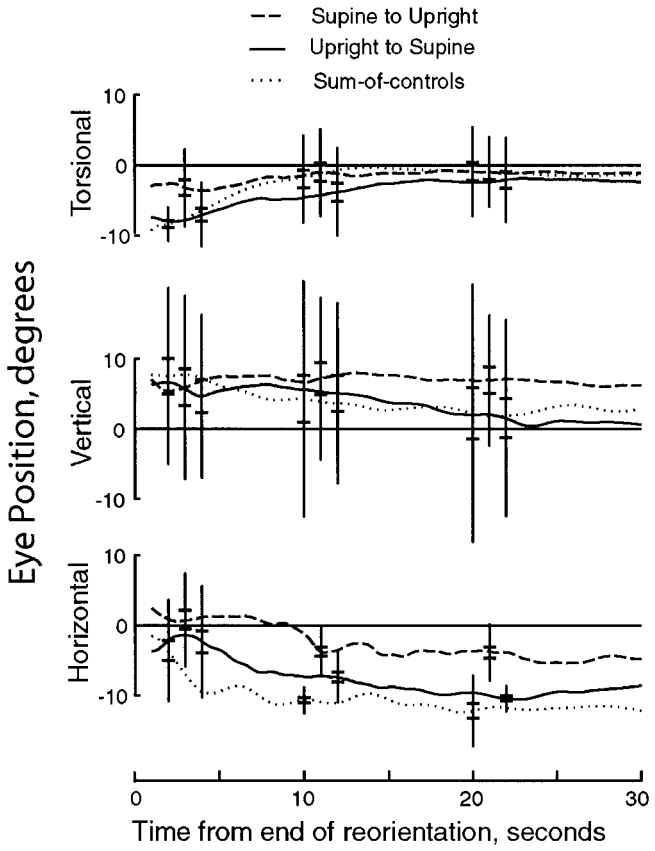

FIG. 8. Mean eye position for 5 subjects after pitch reorientation. Torsional, vertical, and horizontal eye positions for individual subjects were first smoothed with a 2-s moving average. Error bars are ±SD, and tick marks show SE.

(sometimes referred to as "dumping of the velocity storage") and the trend for an increase in peak velocity that was caused by the reorientation of the subject during the on-going rotation about the earth-vertical axis.

However, only small changes to the structure of the model were necessary to get a good correspondence between experimental and simulated data. The first modifications were made to reflect the different gains and time constants for horizontal, vertical, and torsional eye movements, which previously were treated identically. In the original model, velocity storage and angular VOR gain is set by a single parameter in the first feedback loop (k_ω). To account for the observed variation in the time constant of the decay of nystagmus, we allowed the vestibular negative feed back loop for the aVOR to have separate gain parameters k_ω for torsional, vertical, and horizontal eye movements. The location of k_ω was moved into the feedback loop and so makes it possible to abolish the velocity storage without eliminating the open-loop response, as has been done in lesion experiments (Katz et al. 1991; Wearne et al. 1997). The different gain values for the horizontal, vertical, and torsional components were incorporated by using different k_{out} values for the three components. Notice that these changes did not introduce any new free parameters: the decay time of the initial horizontal, vertical, or torsional eye velocity response during the *control* trials determined the corresponding value of k_ω, and the observed eye velocity gain fixed the corresponding k_{out} value.

To include the experimentally observed *dumping* of eye velocity, we introduced a new dumping element in the feedback loop (dump-box in Fig. 9). We used the magnitude of the mismatch signal between the sensed and the expected direction of the gravito-inertial acceleration (output of S_{oto} and $\hat{S}_{\text{oto}}$, respectively) to dump velocity storage. In Fig. 9, this is indicated by the shadowed line from the output of $k_{f\omega}$ to the dumping box. The dumping of the velocity storage is mediated through the empirically determined sigmoid function

$$dump(\omega) = (1 - \text{a}) * \text{e}^{-(b*\omega)^2} + a$$

which induces no change when there is no mismatch but reduces the feedback of the estimated velocity ($\hat{\omega}$) to a for a large mismatch. b determines the speed of the decay. Because the vector $\vec{\omega}$ is three dimensional, its length is given by $\omega = \sqrt{\omega_x^2 + \omega_y^2 + \omega_z^2}$.

After setting the gain-parameters for the aVOR (k_ω and k_{out}) to match our control data, we manipulated the other parameters of the model, notably those that affect the amount of cross coupling between the otoliths and vestibular signals, to try to match simultaneously our reorientation data as well as the OVAR data of Haslwanter et al. (2000).

We chose the time constant for the mechanical transfer function of the canals based on the shortest time constant observed in our control experiments (4.5 s, for torsional eye movements). This time constant is consistent with the model-based results of Dai et al. (1999). S_{oto} is given by the identity matrix plus a constant small acceleration of 0.25 g along the dorsoventral axis. The following additional parameters produced good agreement with our experimental paradigm, as well as OVAR: $\tau_{\text{d}} = 4.5$ s, $\tau_{\text{a}} = 190$ s, $k_{\text{f}\omega} = 0.6$, $k_{\text{f}} = 8$, k_ω(tor/ver/hor) = (0.25/0.7/2.65); $\tau_{\text{leaky}} = 2$ s (= τ in Fig. 9), $\tau_{\text{high-pass}} = 0.33$ s (the transfer function of the "highpass-filter" in Fig. 9 is $\frac{\tau_{high-pass}s}{\tau_{high-pass}s + 1}$), k_{out}(tor/ver/hor) = (0.45/0.95/1.7). The vestibular transfer function is given by $S_{SCC} = \frac{\tau_d s}{\tau_d s + 1}\frac{\tau_a s}{\tau_a s + 1}$, and its internal estimation by $\hat{S}_{SCC} = \frac{\tau_d s}{\tau_d s + 1}$. For the dumping function, a =0.6, and b = 0.55.

Figures 4 and 7 include the exponential fits to the model data. The model produces the decrease in vertical and horizontal time constants and increase in peak velocity observed in our data.

DISCUSSION

Cue-conflict resolution in the VOR

Multi-axis rotations that produce a large conflict between canal and otolith signals result in a decrease in velocity storage. This happens not only for reorientations where the static otolith signal contradicts the rotation signal from the semicircular canals (e.g., horizontal in the upright-to-RED) but also when there is no conflict (e.g., horizontal in the RED-to-upright, where the horizontal velocity signal from the canals is consistent with the constant upright orientation indicated by the otoliths). The conflict between the axis of eye velocity and otolith information induces the system to discard *any* velocity storage not just the velocity storage along the conflicting axis, thus reducing the conflict between otolith and the semicircular

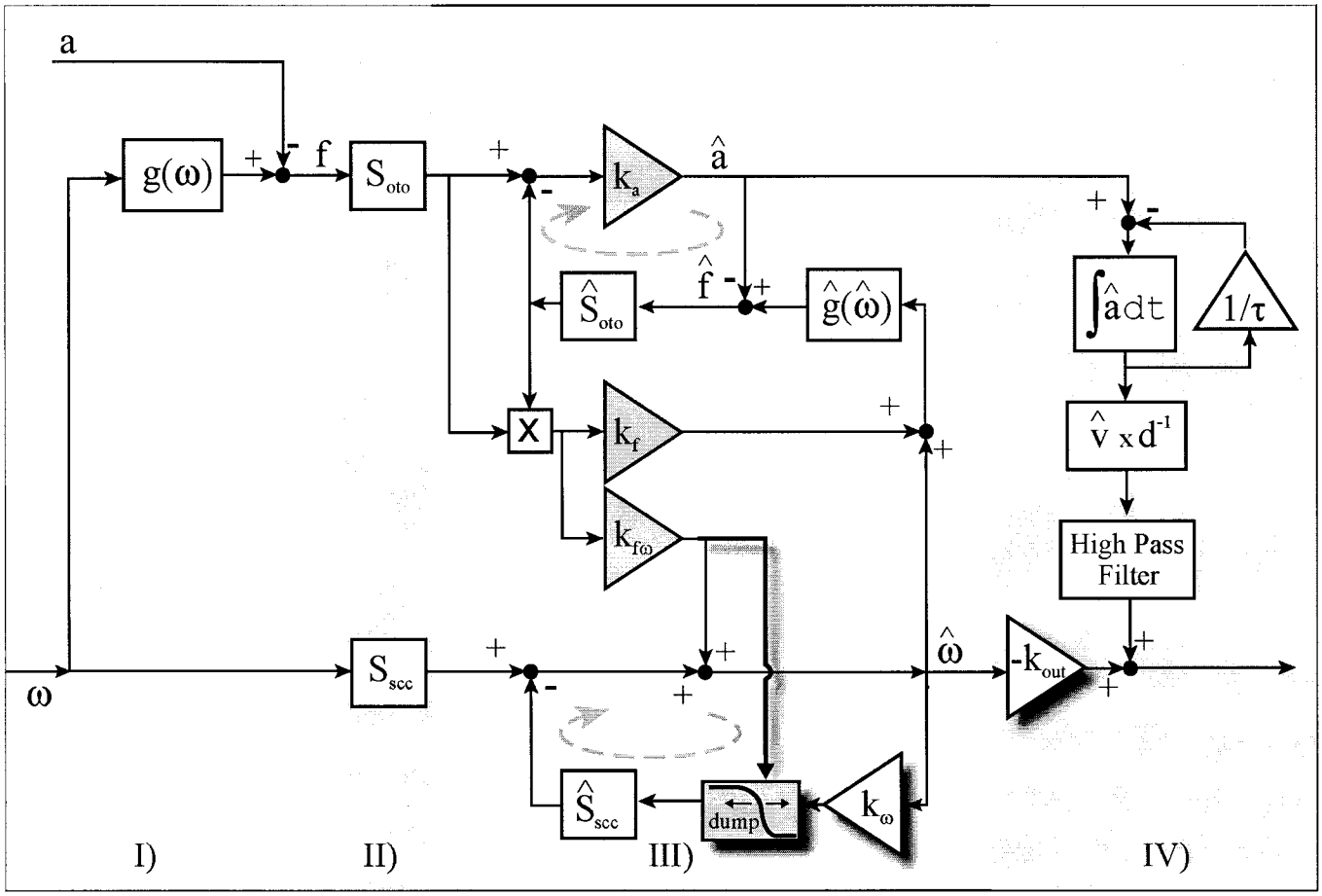

FIG. 9. Otolith-canal interaction model, adapted from Haslwanter et al. (2000). Elements that have been changed with respect to that model have a *black shadow*. Elements that contain parameters that we adjusted to fit the reorientation data are in gray. From left to right, the panels represent: I, movement in space; II, transduction by otoliths and canals; III, internal processing; and IV, eye movement generation. ω, angular velocity vector; a, linear velocity vector; g(ω), update of the current direction of gravity, based on the formula "$dg/dt = g \times \omega$"; S_{scc}, transfer function of the semicircular canals; S_{oto}, transfer function of the otoliths, including a constant pitch-shear force component along the utricular plane; $\times$, vector cross product; k_i, gain factors: k_a, linear acceleration; k_f, adjustment of the perceived direction of gravity; $k_{f\omega}$, cross coupling between linear acceleration and perceived angular movements; k_ω, controls the time constant of the horizontal, vertical, and torsional aVOR; k_{out}, gain of the horizontal, vertical, and torsional aVOR; v, linear velocity; d^{-1}, inverse gaze direction; τ , time constant of the leaky integrator. ˆ, estimated values; e.g., $\hat{\omega}$ is the estimated angular velocity. The values for all the parameters, as well as the transfer functions and the dumping function, are given in the text.

canal signals (Merfeld et al. 1993b). We also found a trend for peak velocity to increase after reorientation. Our modeling, discussed in the following text, suggests this might arise due to the suppression of velocity storage.

The small but significant reduction of the vertical time constant after reorientation demonstrates that there is some vertical velocity storage, albeit less than in the horizontal component. While the mechanical time constant for the canals has never been explicitly measured in humans, our experimental results are consistent with the model-based approach of Dai et al. (1999), who estimated that the human cupula time constant is between 3.5 and 7 s. No reduction in the time constant of torsional nystagmus was found, though we did find an increase in peak velocity.

Our finding of small reorienting effects is similar to that of Fetter et al. (1996): they reoriented human subjects after the cessation of an earth-vertical axis rotation and found only small realignments of the axis of eye velocity. By comparing the decay time constants, we observed a statistically significant reorientation of eye velocity in the pitch reorientation experiment and a nonsignificant trend for reorientation of the eye-velocity axis toward upright in the roll experiment. In both cases, we only observed the effect when subjects were tilted to upright, and in neither case did the axis of eye velocity align with the head-velocity axis until eye velocity was very small. In monkey, this behavior is considerably enhanced, suggesting that the otolith signals are used to modify semi-circular canal signals and so provide a gravity-based reference frame for the VOR (Angelaki and Hess 1994; Merfeld et al. 1993b). In humans, we suggest that the general dumping of velocity storage in response to the cue conflict largely suppresses the reorienting behavior. The axis of eye velocity also reorients toward gravity in humans when the information about head rotation is visual, that is, during optokinetic nystagmus (OKN) (Gizzi et al. 1994). This reorientation effect is considerably smaller than in monkey (Cohen et al. 1999). Because the gain of OKN is generally smaller than the gain of vestibular nystagmus, it is also possible that reorientation is only apparent

with weaker head rotation stimuli, when the conflict with the otolith information is smaller.

In quite a different study on the effects of low-frequency otolith stimulation on eye movements, Bockisch and Haslwanter (2001) found that static head pitch and tilt position had smaller effects on 3D eye position in human than monkey. In that experiment, fixation eye positions were measured so the differences in otolith mediated eye movements between primates do not only reflect differences in the velocity-storage mechanism. In general, it appears that low-frequency otolith stimulation has considerably smaller effects on human eye movements than on monkey eye movements. At higher frequencies, however, humans show robust otolith-ocular reflexes that help to compensate for the retinal slip caused by fast linear movements (Baloh et al. 1988; Paige 1989).

Conflicts between the otoliths and the canals as large as those studied here are not likely to occur naturally, but smaller conflicts presumably occur due to age- and disease-related changes in the vestibular-ocular system. However, paradigms similar to ours have been of interest in aerospace physiology, where the spatial disorientation and nausea induced by conflict stimuli could affect pilot and astronaut performance (Benson and Bodin 1966; DiZio and Lackner 1988; DiZio et al. 1987; Guedry and Benson 1978). The adaptive mechanisms necessary to compensate for vestibular cue conflicts have received special attention in the context of long-duration space missions (Hecht et al. 2001; Young et al. 2001). The lack of gravity during extended space flights causes many complications, from decalcification of the bones to a decrease in the efficacy of the autoimmune system. To counter these effects, it may be possible to replace gravity with centrifugal force by rotating the space module ("artificial gravity"). In that case, any head movement of a crewmember about an axis that does not coincide with the rotation axis of the space module would—inappropriately—stimulate the semicircular canals in the same way they are stimulated during reorientations in the study presented here. Hecht et al. (2001) asked subjects to make 90° yaw-head movements while supine on a short-axis centrifuge, and, similar to our results, they found that the eye movements corresponded well with predictions based only on semi-circular canal responses. (Because in our control experiments the orientation with respect to gravity was constant, the control data essentially provides a canal-only prediction.) The experiments by Hecht et al. also showed that the vestibular-ocular system can further reduce the amount of inappropriate eye movements if visual information is also available: multiple executions of head movements in the light during rotation on a short-arm centrifuge, repeated over a number of days, can induce a reduction of the gain of the inappropriate eye velocity (Young et al. 2001). This adaptation shows large intersubject variability and may also be quite context specific.

Neurophysiologic significance

Physiologic control of the behaviors reported here (dumping of velocity storage, reorientation of the axis of eye velocity when subjects tilt to upright) seems to require, at least, convergence of sensory signals from the otolith organs to structures related to the velocity-storage mechanisms. The nodulus and uvula are likely candidate regions because electrical stimulation of the these regions in monkeys reduces the horizontal time constant elicited with both vestibular and optokinetic stimuli (Solomon and Cohen 1994). Further, complete lesions of these regions eliminates the dumping of horizontal velocity storage during cue-conflicts caused by postrotatory tilts or visual stimulation (Angelaki and Hess 1995; Waespe et al. 1985; Wearne et al. 1998). Separate lesions of the central and lateral regions of the nodulus and uvula further suggest that the lateral portions control horizontal velocity storage, while central portions control vertical and torsional velocity storage (Wearne et al. 1998). The reorientation of the axis of eye velocity toward gravity observed in monkeys, and suggested in our studies when subjects were tilted toward upright, also depends on intact nodulus and uvula (Angelaki and Hess 1995; Wearne et al. 1998).

We interpret the dumping of velocity storage after reorientation as arising from a process of resolving the cue conflict between head-rotation signals from the vestibular canals and head-orientation information from the otoliths. For two reasons, canal-canal interaction is not likely to be a significant source of the dumping: first, the rotations indicated by the three canals do not lead to an inherent contradiction, and second, velocity storage dumping after postrotatory reorientation still occurs even in monkeys with the lateral or posterior canals inactivated due to plugging (Angelaki and Hess 1995).

Our results also make specific predictions about realistic implementations of velocity storage, which theoretically can be realized in a number of different ways. In our model, it was implemented as a *negative* feedback loop that contains an estimate of the peripheral canal/otolith transfer function. Dumping the velocity storage reduces the negative feedback, thereby increasing the maximum eye velocity. It is also possible to extend the time constant of the velocity decay through a *positive* feedback of a low-pass filtered angular velocity signal. However, elimination of such a positive feedback would decrease the maximum velocity of the eye-movement response in contrast to the observed trend for an increase. Other models implement velocity storage by addition of a "direct" pathway, with no velocity storage, and an "indirect" pathway, through a leaky integrator (Dai et al. 1999; Raphan et al. 1979). But again, selectively suppressing the indirect pathway in this sort of model would also necessarily decrease peak eye velocity, which is not consistent with our data. The dumping of the velocity storage together with the simultaneous increase in eye velocity found in our experiments suggests that velocity storage is implemented through a negative feedback loop.

The coupling of time constant and peak velocity in the model is consistent with the results of lesion experiments in rhesus monkeys (Wearne et al. 1997). Midline section of the rostral medulla abolished all oculomotor functions related to velocity storage and also tended to increase the VOR gain (Wearne et al. 1997). In a different experiment, Katz et al. (1991) found no change in VOR gain after velocity-storage elimination by midline medullary lesions. The reason for this discrepancy may be that adaptive gain mechanisms, which were found to be intact in these animals, reduced the aVOR gain after surgery.

Canal-otolith interaction model

Our model of canal-otolith interaction, which is based on suggestions by Merfeld (Merfeld 1995; Merfeld et al. 1993a),

fit our data as well as the OVAR results of Haslwanter et al. (Haslwanter et al. 2000). Including the dumping of velocity storage explained the experimentally observed decrease in the time constant of nystagmus and the trend for an increase in the maximum velocity for all types of reorientation. Without the dumping mechanism, the model could not simultaneously fit both the OVAR data and our reorientation data: reproducing the reorientation data required an increase in the cross-coupling between the otoliths and the canals, which produced eye-velocity modulation during OVAR that was substantially too large. Likewise, parameters that fit the OVAR data resulted in minimal dumping of the velocity storage after reorientation. Although we did not include it in the model here, the framework allows for dumping by other sensory mismatches. For example, visual input during postrotatory nystagmus could also be used to drive the velocity-dumper.

Because the reorientation of the axis of eye velocity to upright was small in our data, we opted not to account for it in the model. Thus our model is specific for the main features of human canal-otolith interaction observed here and during OVAR (Haslwanter et al. 2000) and cannot account for data from postrotatory tilt studies in monkey, where the axis of eye velocity aligns with gravity (Angelaki and Hess 1994; Merfeld et al. 1993b). The Angelaki and Hess model, which does explain the postrotatory tilt data in monkeys, is quite specific for that stimulus and does not reproduce the generation of linear VOR by otolith stimulation (Angelaki and Hess 1995).

We thank R. Jaeger for implementing the original canal-otolith interaction model, A. Züger for technical assistance, and Dr. L. Young for valuable comments.

This work was supported by the Swiss National Science Foundation (3231-059838.97/3200-052187.97 and 31-63669.00), the Betty and David Koetser Foundation for Brain Research, the Hartmann-Müller Foundation, the EMDO-Foundation, and the Olga-Mayenfisch-Foundation.

REFERENCES

Angelaki DE and Hess BJ. Inertial representation of angular motion in the vestibular system of rhesus monkeys. I. Vestibuloocular reflex. *J Neurophysiol* 71: 1222–1249, 1994.

Angelaki DE and Hess BJ. Inertial representation of angular motion in the vestibular system of rhesus monkeys. II. Otolith-controlled transformation that depends on an intact cerebellar nodulus. *J Neurophysiol* 73: 1729–1751, 1995.

Angelaki DE and Hess BJ. Three-dimensional organization of otolith-ocular reflexes in rhesus monkeys. II. Inertial detection of angular velocity. *J Neurophysiol* 75: 2425–2440, 1996.

Baloh RW, Beykirch K, Honrubia V, and Yee RD. Eye movements induced by linear acceleration on a parallel swing. *J Neurophysiol* 60: 2000–2013, 1988.

Benson AJ and Bodin MA. Comparison of the effect of the direction of the gravitational acceleration on post-rotational response in yaw, pitch and roll. *Aerosp Med* 37: 889–897, 1966.

Bockisch CJ and Haslwanter T. 3D eye position during static roll and pitch in humans. *Vision Res* 41: 2127–2137, 2001a.

Bockisch CJ, Straumann D, and Haslwanter T. Eye movements during mult-axis rotations. *Soc Neurosci Abstr* 27: 298.18, 2001.

Bockisch CJ, Straumann D, and Haslwanter T. Oculomotor responses to multi-axis rotations. *11th Annual Meeting of the Society for the Neural Control of Movement.* Sevilla, Spain, 6, C13. 2001b.

Cohen B, Wearne S, Dai M, and Raphan T. Spatial orientation of the angular vestibulo-ocular reflex. *J Vestib Res* 9: 163–172, 1999.

Dai M, Klein A, Cohen B, and Raphan T. Model-based study of the human cupular time constant. *J Vestib Res* 9: 293–301, 1999.

Darlot C, Denise P, Droulez J, Cohen B, and Berthoz A. Eye movements induced by off-vertical axis rotation (OVAR) at small angles of tilt. *Exp Brain Res* 73: 91–105, 1988.

DiZio P and Lackner JR. The effects of gravitoinertial force level and head movements on post-rotational nystagmus and illusory after-rotation. *Exp Brain Res* 70: 485–495, 1988.

DiZio P, Lackner JR, and Evanoff JN. The influence of gravitoinertial force level on oculomotor and perceptual responses to coriolis, cross-coupling stimulation. *Aviat Space Environ Med* 58: A218–A223, 1987.

Fetter M, Heimberger J, Black RA, Hermann W, Sievering F, and Dichgans J. Otolith-semicircular canal interaction during postrotatory nystagmus in humans. *Exp Brain Res* 108: 463–472, 1996.

Fetter M, Tweed D, Hermann W, Wohland-Braun B, and Koenig E. The influence of head position and head reorientation on the axis of eye rotation and the vestibular time constant during postrotatory nystagmus. *Exp Brain Res* 91: 121–128, 1992.

Gizzi M, Raphan T, Rudolph S, and Cohen B. Orientation of human optokinetic nystagmus to gravity: a model-based approach. *Exp Brain Res* 99: 347–360, 1994.

Glasauer S and Merfeld DM. Modeling three-dimensional vestibular responses during complex motion stimulation. In: *Three-Dimensional Kinematics of Eye, Head and Limb Movements,* edited by Fetter M, Haslwanter T, Misslisch H, and Tweed D. Amsterdam: Harwood Academic, 1997, p. 387–398.

Guedry FE and Benson AJ. Coriolis cross-coupling effects: disorienting and nauseogenic or not? *Aviat Space Environ Med* 49: 29–35, 1978.

Hain TC, Ramaswamy TS, and Hillman MA. Anatomy and physiologoy of the normal vestibular system. In: *Vestibular Rehabilitation,* edited by Herdman SJ. Philadelphia, PA: Davis, 2000, p. 3–24.

Harris LR. Vestibular and optokinetic eye movements evoked in the cat by rotation about a tilted axis. *Exp Brain Res* 66: 522–532, 1987.

Haslwanter T. Mathematics of three-dimensional eye rotations. *Vision Res* 35: 1727–1739, 1995.

Haslwanter T, Curthoys IS, Black RA, Topple AN, and Halmagyi GM. The three-dimensional human vestibulo-ocular reflex: response to long-duration yaw angular accelerations. *Exp Brain Res* 109: 303–311, 1996.

Haslwanter T, Jaeger R, Mayr S, and Fetter M. Three-dimensional eye-movement responses to off-vertical axis rotations in humans. *Exp Brain Res* 134: 96–106, 2000.

Hecht H, Kavelaars J, Cheung CC, and Young LR. Orientation illusions and heart-rate changes during short-radius centrifugation. *J Vestib Res* 11: 115–127, 2001.

Helmholtz H. *Handbuch der Physiologischen Optik.* Leipzig: Voss, 1867.

Hepp K. On Listing's law. *Commun Math Phys* 132: 285–292, 1990.

Hess BJ and Dieringer N. Spatial organization of the maculo-ocular reflex of the rat: responses during off-vertical axis rotation. *Eur J Neurosci* 2: 909–919, 1990.

Imai T, Moore ST, Raphan T, and Cohen B. Interaction of the body, head, and eyes during walking and turning. *Exp Brain Res* 136: 1–18, 2001.

Katz E, Vianney de Jong JM, Buettner-Ennever JA, and Cohen B. Effects of midline section on the velocity storage and the vestibulo-ocular reflex. *Exp Brain Res* 87: 505–529, 1991.

Merfeld D. Modeling human vestibular responses during eccentric rotation and off vertical axis rotation. *Acta Otolaryngol* 520: 354–359, 1995.

Merfeld D, Young LR, Oman CM, and Shelhamer M. A multidimensional model of the effect of gravity on the spatial orientation of the monkey. *J Vestib Res* 3: 141–161, 1993a.

Merfeld DM, Young LR, Paige GD, and Tomko DL. Three dimensional eye movements of squirrel monkeys following postrotatory tilt. *J Vestib Res* 3: 123–139, 1993b.

Merfeld DM, Zupan L, and Peterka RJ. Humans use internal models to estimate gravity and linear acceleration. *Nature* 398: 615–618, 1999.

Misslisch H and Hess BJ. Three-dimensional vestibuloocular reflex of the monkey: optimal retinal image stabilization versus Listing's Law. *J Neurophysiol* 83: 3264–3276, 2000.

Misslisch H and Tweed D. Neural and mechanical factors in eye control. *J Neurophysiol* 86: 1877–1883, 2001.

Misslisch H, Tweed D, Fetter M, Dichgans J, and Vilis T. Interaction of smooth pursuit and the vestibuloocular reflex in three dimensions. *J Neurophysiol* 75: 2520–2532, 1996.

Misslisch H, Tweed D, Fetter M, Sievering D, and Koenig E. Rotational kinematics of the human vestibuloocular reflex. III. Listing's Law. *J Neurophysiol* 72: 2490–2502, 1994.

Paige GD. The influence of target distance on eye movement responses during vertical linear motion. *Exp Brain Res* 77: 585–593, 1989.

Raphan T, Cohen B, and Henn V. Effects of gravity on rotatory nystagmus in monkeys. *Ann NY Acad Sci* 374: 44–55, 1981.

Raphan T, Matsuo V, and Cohen B. Velocity storage in the vestibulo-ocular reflex arc (VOR). *Exp Brain Res* 35: 229–248, 1979.

Schmid-Priscoveanu A, Straumann D, and Kori A. Torsional vestibulo-ocular reflex during whole-body oscillation in the upright and the supine position. I. Responses in healthy human subjects. *Exp Brain Res* 134: 212–219, 2000.

Solomon D and Cohen B. Stimulation of the nodulus and uvula discharges velocity storage in the vestibulo-ocular reflex. *Exp Brain Res* 102: 57–68, 1994.

Straumann D. Off-line computing of slow-phase eye velocity profiles evoked by velocity steps or caloric stimulation. *Int J Biomed Comput* 29: 61–65, 1991.

Straumann D, Zee DS, Solomon D, Lasker AG, and Roberts DC. Transient torsion during and after saccades. *Vision Res* 35: 3321–3334, 1995.

Tweed D, Cadera W, and Vilis T. Computing three-dimensional eye position quaternions and eye velocity from search coil signals. *Vision Res* 30: 97–110, 1990.

Tweed D, Sievering D, Misslisch H, Fetter M, Zee D, and Koenig E. Rotational kinematics of the human vestibuloocular reflex. I. Gain matrices. *J Neurophysiol* 72: 2467–2479, 1994.

Tweed D and Vilis T. Geometric relations of eye position and velocity vectors during saccades. *Vision Res* 30: 111–127, 1990.

Waespe W, Cohen B, and Raphan T. Dynamic modification of the vestibulo-ocular reflex by the nodulus and uvula. *Science* 228: 199–202, 1985.

Wearne S, Raphan T, and Cohen B. Contribution of vestibular commissural pathways to spatial orientation of the angular vestibuloocular reflex. *J Neurophysiol* 78: 1193–1197, 1997.

Wearne S, Raphan T, and Cohen B. Control of spatial orientation of the angular vestibuloocular reflex by the nodulus and uvula. *J Neurophysiol* 79: 2690–2715, 1998.

Wilson VJ and Jones Melvill G. *Mammalian Vestibular Physiology.* New York: Plenum, 1979.

Young LR, Hecht H, Lyne LE, Sienko KH, Cheung CC, and Kavelaars J. Artificial gravity: head movements during short rotation radius centrifugation. *Acta Astronautica* 49: 215–226, 2001.